AD-A037 861

PERSON (LEIF N) TRONDHEIM (NORWAY)
ON SHOCK WAVES IN ROCK CREATED BY SURFACE-AND NEAR-TO-SURFACE-D--ETC(U)
JAN 77   L N PERSEN   F44620-75-C-0029
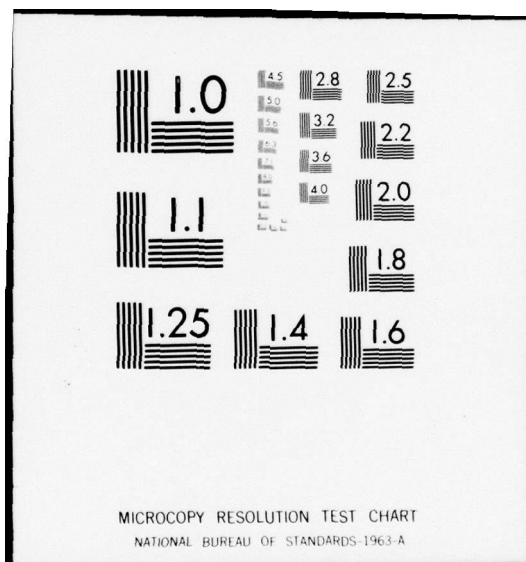
F/G 8/11

UNCLASSIFIED   SCIENTIFIC-2   AFGL-TR-77-0070   NL

| OF
ADA037861

END

DATE
FILMED

4-77

MICROCOPY RESOLUTION TEST CHART
NATIONAL BUREAU OF STANDARDS-1963-A

AFGL-TR-77-0070

ON SHOCK WAVES IN ROCK CREATED BY
SURFACE- AND NEAR-TO-SURFACE-DETONATIONS

Leif N. Persen

Institute of Applied Mechanics,
University of Trondheim, NTH, 7034
Trondheim, Norway

Scientific Report No. 2

31 January 1977

D D C
APR 4 1977
C

AIR FORCE GEOPHYSICS LABORATORY
AIR FORCE SYSTEMS COMMAND
UNITED STATES AIR FORCE
HANSCOM AFB, MASSACHUSETTS 01731

Qualified requestors may obtain additional copies from the Defense
Documentation Center. All others should apply to the National
Technical Information Service.

REPORT DOCUMENTATION PAGE		READ INSTRUCTIONS BEFORE COMPLETING FORM
1. REPORT NUMBER AFGL-TR-77-0070	2. GOVT ACCESSION NO.	3. RECIPIENT'S CATALOG NUMBER
4. TITLE *(and Subtitle)* ON SHOCK WAVES IN ROCK CREATED BY SURFACE- AND NEAR-TO-SURFACE-DETONATIONS		5. TYPE OF REPORT & PERIOD COVERED Scientific Report No. 2
		6. PERFORMING ORG. REPORT NUMBER
7. AUTHOR(s) Leif N. Persen Professor, Insitute of Applied Mechanics, University of Trondheim, NTH, 7034 Trondheim		8. CONTRACT OR GRANT NUMBER(s) F44620-75-C-0029
9. PERFORMING ORGANIZATION NAME AND ADDRESS Leif N. Persen, Oscar Wistings vei 20B Trondheim 70000 Norway		10. PROGRAM ELEMENT, PROJECT, TASK AREA & WORK UNIT NUMBERS 76391301
11. CONTROLLING OFFICE NAME AND ADDRESS European Office of Aerospace Research and Development, (AFSC), 223/231 Old Marylebone Road, London NW 1 5th, England		12. REPORT DATE 77 Jan 31
		13. NUMBER OF PAGES 36
14. MONITORING AGENCY NAME & ADDRESS*(if different from Controlling Office)* Air Force Geophysics Laboratory(LWW) Hanscom AFB, Massachusetts 01731 Monitor/Ker Thomson/LWW		15. SECURITY CLASS. *(of this report)* Unclassified
		15a. DECLASSIFICATION/DOWNGRADING SCHEDULE

16. DISTRIBUTION STATEMENT *(of this Report)*

Approved for public release: distribution unlimited.

17. DISTRIBUTION STATEMENT *(of the abstract entered in Block 20, if different from Report)*

18. SUPPLEMENTARY NOTES

This report appears as a supplement to and an integral part of the Final Report: THE APPLICATION OF THEORETICAL RESULTS IN THE DESIGN OF SAFE SHELTERS IN ROCK by Leif N. Persen

19. KEY WORDS *(Continue on reverse side if necessary and identify by block number)*

Wave propagation in rock, Cratering, Surface bursts

20. ABSTRACT *(Continue on reverse side if necessary and identify by block number)*

A review is given of the research efforts sponsored by the German Defense Ministry to investigate the problem of coupling at surface bursts exprimentally. Some results from the CENSE I experiments are also called to attention. The cratering process is connected to the evaluation of confined explosions.

DD FORM 1473 EDITION OF 1 NOV 65 IS OBSOLETE
1 JAN 73

388849

- I -

CONTENTS

On Shock Waves in Rock Created by
Surface- or Near-to-Surface Detonations

by
Leif N. Persen

1.Introduction.

This presentation is aimed at giving a survey of the
small scale experiments performed in Norway on behalf of the West-
German Defense Ministry to start a research activity in the field
covered by the title of this report. In addition the data from the
CENSE experiments, which were obtained with much larger charges,
are drawn upon to see if conclusions from the first set of data
could be substantiated. The small scale experiments have been re-
ported on in [1], the CENSE experiment is covered in [2], and the
data from the latter have been obtained directly from the record-
ings. In addition results from some earlier experiments are drawn
to attention. These have been treated separately in [3].

2.General remarks.

The general philosophy behind the small scale experi-
ments referred to above can be outlined as follows. Usually the
rock site of an installation has been tested by confined explo-
sions. In this way the properties of the rock site as a transmitt-
ing medium may be considered known, for instance in the way descri-
bed in [3]. Consequently the creation of a shock wave and its trans-
mission through the rock may be said to be well known, provided the
magnitude of the creating charge is known, and that it is detonated
fully confined.

In the case of a shelter of some kind, the charge
creating the shock wave is usually considered to be a surface
charge of some sort. Detonation is supposed to take place above
ground level, on the ground or at a certain penetation depth be-
neath the surface. The problem then arises how to make predictions
for the propagation of the created shock wave based only on the

knowledge of the fully confined case. One way of answering this question is to perform exeriments whereby the position of the charge above (or beneath) the surface is changed from one detonation to another, each time observing the created shock wave. This idea was more or less the basis for the CENSE experiments, and the result came out as diagrams of the "containment factors" for different quantities.

The small scale experiments were based on a somewhat more sophisticated philosophy. As shown in [3], pp.192-194, a possibility exists to draw direct conclusions for socalled "half burried" cases from knowledge of the fully contained case. It was therefore thought sufficient to relate cases with varying heights of the detonating charge above the surface to the "half burried" case. In this way the problem was split in two "stages", each stage being basically different from the other as the physics indicate. For positions of the charge on or close to but beneath the surface cratering becomes a problem. For positions of the charge above the surface cratering does not necessarily take place. It seems realistic to treat these two "stages" separately.

3.The experiment Vikersund.

A small scale experiment were performed in VIKERSUND, Norway. Two different geometries were used. The first one is shown in Fig.1 . A natural precipice with a rather un-eroded surface was located. In front of or at the vertical wall the charges were detonated at A. From the top of the precipice the holes 1 - 9 were drilled so that the pick-ups used for measuring strain or particle acceleration as the shock wave was transmitted could be positioned in the rock. All measuring devices were placed on the perpendicular to the surface at A. A separate hole was drilled so that a confined charge could be detonated in B. This made it possible to monitor the shock wave as it travelled in both directions between A and B, and thereby eventual systematical deviations could be detected. This part of the experiment was more or less a repetition of the experiment described in [3], pp 175-194.
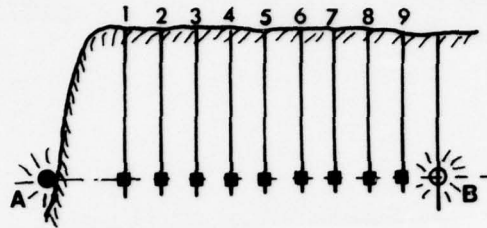
*Fig.1. Geometry of the "row"-experiment
at VIKERSUND, Norway.*

In the second geometry used at VIKERSUND, the tech-
nique of fixing strain gauge directly to the rock was used. A hole
was drilled normal to the surface of the rock as shown in Fig.2 .
Strain gauges were fixed to the rock surface at different distances
in the hole from the surface. The necessary wiring was led away in
a sloping hole to prevent it from being broken by the explosion.
The hole is then filled with concrete, and it was hoped that the
signals would give a direct measurement of the strain in the rock
during the passage of the shock wave. The shock wave was created
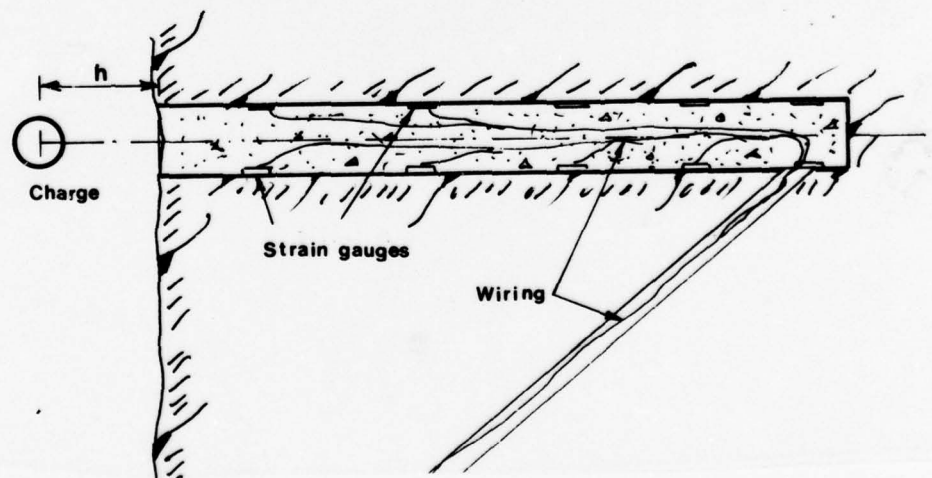
Fig.2. Geometry of the "hole"-experiment at VIKERSUND, Norway.

by letting a charge be detonated as shown, whereby the distance h
and the charge magnitude W were varied from case to case. The re-
sults from these experiments will be treated separately.

4.The "row"-experiment, VIKERSUND.

In the "row"-experiment only charges in contact with
the surface of the rock at A in Fig.1 were detonated. Consequently
an increasing crater was developing at A as the experiment progress-
ed. Because the magnitude W of the charge was increased gradually,
one operated almost automatically with "half burried" charges.

The shots were numbered consequtively, and Table I
shows how the charge magnitude was changed. The table also give
the maximum amplitude of the shock wave measured in [μ-strain] at
each of the nine pickups. These details are given to illustrate
the repeatability of the measurements. As shown the repeatability
is not as good as one could wish, and each signal from each pickup
was therefore scrutinized for "misbeaviour" which might indicate
decreased reliability. It was found that only the shots A4,A5,A6,
A11,A12 and A14 could be used with some confidence. The fully con-

TABLE I			Maximum amplitude A_i[μ-strain]								
Shot		W	measured at pickup No:								
in	No.	[kg]	i=1	2	3	4	5	6	7	8	9
B	1	0,5	61	83	131	190	157	183	256	610	792
B	2	2.0	58	71	71	131	–	–	214	490	875
A	3	0.5	792	238	–	–	–	–	–	–	–
A	4	0,5	582	155	22	21	11	9	–	–	–
A	5	0,5	629	190	36	34	15	12	–	22	17
A	6	2,0	1780	547	155	131	45	42	21	(32)	29
A	7	2,0	1466	309	(27)	42	20	16	–	18	12
A	8	2,0	–	285	95	98	46	36	–	41	24
B	9	2,0	23	36	60	131	78	131	250	626	933
A	10	5,0	1982	1368	268	–	–	–	–	128	63
A	11	5,0	–	893	190	238	76	58	59	85	51
A	12	15,0	–	2320	690	547	218	204	140	321	168
A	13	15,0	–	2507	489	319	171	148	154	294	139
A	14	30,0	–	4160	1082	786	278	296	357	514	274
A	42	30,0	–	4047	1071	785	171	185	330	350	245

tained shot B1, B2 and B9 will be treated separately, as these are
giving the reference frame for the wave propagation for this par-

ticular rock. (the norwegian "Gneis").

The arrival times for each signal at each pickup was used to determine the signal velocity in the rock. Because the positions of the pickups are known, the arrival times t_i may be
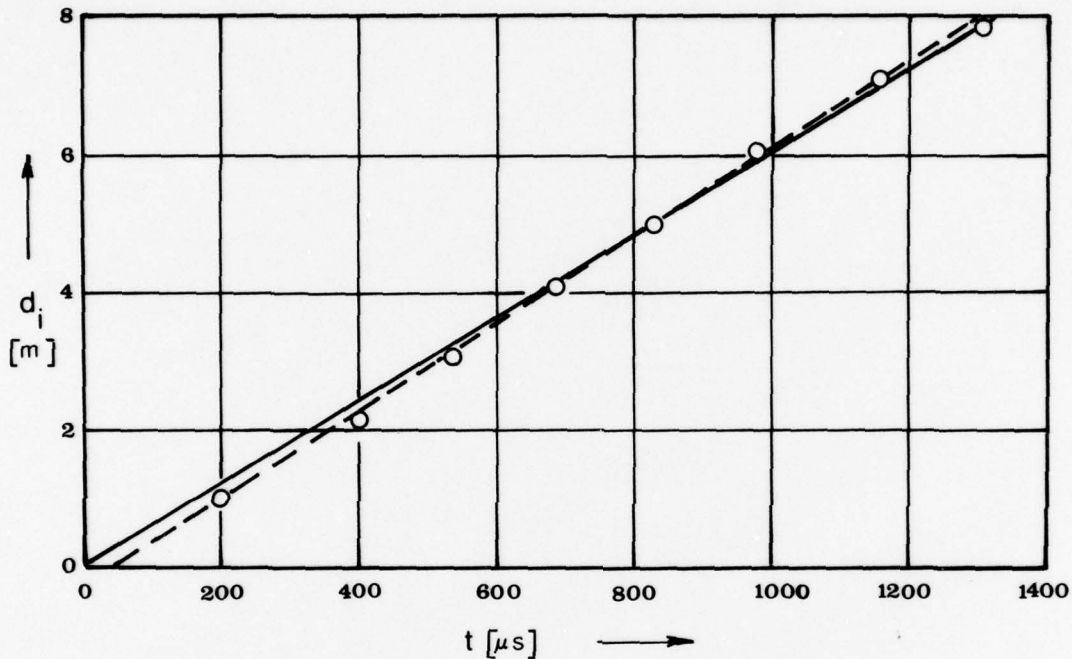
Fig.3. Arrival times t_i plotted as function of the distance d_i

plotted as a function of the distance d_i of each pickups from the point of detonation A, as shown in Fig. 3. The slope of the straight line through the points will then give the signal velocity c_s of the rock. Now there are two possibilities for defining this line:

$$\text{either:} \quad d = d_o + c_s t \tag{4.1}$$

$$\text{or:} \quad d = c_s t \tag{4.2}$$

Linear regression gives:

$$\text{either:} \quad c_s = 6327 \text{ [m/s]} , \ d_o = 0.27 \text{ [m]} \tag{4.3}$$

$$\text{or:} \quad c_s = 6030 \text{ [m/s]} \tag{4.4}$$

The two cases are illustrated in Fig.3 by a dashed line and a fully drawn line respectively. The difference between the to results amounts to 5%, and the absolute value of c_s is rather high. This rather trivial determination of the signal velocity has been given in detail here because it indicates the quality of the measurements.

The data for the "row"-experiment consists of the maximum amplitude A_i measured at pickup No.i, the dispersion C_i measured as the maximum slope of the signal in it first phase at each pickup, and the distance d_i from the explosion to the pickup. In addition the calibration constant k_i of each pickup may be considered as input data. These are now treated as shown in [3] to obtain the attenuation curves for the maximum amplitude and the dispersion. The whole procedure is given in Tables II and III, where the determination of the shot factors β, the corrected values of the non-dimensional distances $\xi_{i,corr}$ as well as of the charactreistic lenghts a for each shot are also shown. The dispersion data C_i have been made dimensionless using

$$c_s = 6250 \ [\text{m/s}] \quad , \quad p_o = A_o^* \tag{4.5}$$

The attenuation curves will assymptotically be expressible as

$$A = A_o^* \xi^\lambda \quad \text{(for the max. ampl.)} \tag{4.6}$$

$$C = C_o^* \xi^{\lambda_a} \quad \text{(for the dispersion)} \tag{4.7}$$

The evaluation delivers the values of A_o^*, C_o^*, λ and λ_a, with the added information of the standard deviation m given in percent of the measured values.

As mentioned some of the data obtained were rejected leaving only data from 6 of the shots to be considered. To make sure that one has not introduced any irrelevant regularity by this selection, the shots A12 and A14 with the larger charges were also

TABLE III

Shot No.	Pickup i	ε_i corr	c_i [μ-str/μs]	k_i [μ-str/atm]	a [m]	$a \cdot 10^4 / A_o c_e$	$c_i \cdot a / P_o c_e k_i$
A4 0.5 kg	1	16.95	28.7	3.16151	.06607	2.54270	2.309-3
	2*	32.09	4.17	4.86875			2.178-4
	3*	49.64	0.50	3.21412			3.956-5
	4**	63.27	0.46	4.38324			2.668-5
	5**	78.86	0.22	3.33552			1.677-5
	6*	92.33	0.32	3.01506			(2.699-5)
	7			3.15001			
	8						
A5 0.5 kg	1	14.37	31.0	3.16151	.07792	2.99859	2.940-3
	2*	27.21	6.55	4.86875			4.034-4
	3*	42.09	0.86	3.21412			8.024-5
	4**	53.65	0.56	4.38324			3.831-5
	5**	66.86	0.21	3.33552			1.882-5
	6*	78.29	0.32	3.01506			(2.877-5)
	7						
	8						
	9						
A6 2.0 kg	1	8.07	73.3	3.16151	.13882	5.34232	1.293-2
	2*	15.27	19.2	4.86875			2.107-3
	3*	23.63	4.60	3.21412			7.646-4
	4**	30.11	2.96	4.38324			3.602-4
	5**	37.53	0.97	3.33552			1.54-4
	6*	43.94	1.76	3.01506			(3.119-4)
	7		1.05				
	8		0.48				
	9						
A11 5.0 kg	1	12.52	26.0	3.16151	.16933	6.51652	3.480-3
	2*	19.37	4.39	4.86875			8.901-4
	3*	24.69	1.14	3.21412			6.690-4
	4**	30.77	1.37	4.38324			2.227-4
	5**	36.02	7.79	3.33552			(2.96-4)
	6*	42.34	0.63	3.01506			1.303-4
	7	48.49	0.56	3.15001			
	8	53.03	0.46				
	9						
A12 15.0 kg	1	7.59	80.0	3.16151	.27944	1.07541	1.767-2
	2*	11.74	25.0	4.86875			5.522-3
	3*	14.96	15.4	3.21412			3.572-3
	4**	18.64	7.90	4.38324			2.543-3
	5**	21.83	7.79	3.33552			(2.779-3)
	6*	25.66	4.91	3.01506			1.676-3
	7	29.38	7.36	3.15001			
	8	32.14	1.93				
	9						
A14 30.0 kg	1	6.29	143.0	3.16151	.33685	1.29637	3.808-2
	2*	9.74	40.0	4.86875			1.613-2
	3*	12.41	18.2	3.21412			5.385-3
	4**	15.47	8.68	4.38324			3.37-3
	5**	18.11	8.36	3.33552			(9.59-3)
	6*	21.29	6.90	3.01506			2.840-3
	7	24.37	10.40	3.15001			
	8	26.66	3.92	3.22872			
	9			2.89311			

TABLE II

Shot No.	Pickup i	d_i [m]	A_i [μ-strain]	k_i [μ-str/atm]	a [m]	$\varepsilon_{i,corr}$	A_i [atm]	B
A4 0.5 kg	1	1.12	582	3.16151	.066	16.95	(184.09)	5.83987
	2*	2.12	155	4.86875		32.09	31.84	
	3*	3.28	22	3.21412		49.64	6.84	
	4**	4.18	21	4.38324		63.27	4.79	
	5**	5.21	11	3.33552		78.86	3.30	
	6*	6.10	9	3.01516		92.33	2.99	
	7	7.17	-	3.15001		-	-	
	8	8.21	-	3.22872		-	-	
	9	8.98	-	2.89311		-	-	
A5 0.5 kg	1	1.12	629	3.16151	.078	14.37	(198.96)	4.09469
	2*	2.12	190	4.86875		27.21	39.02	
	3*	3.28	36	3.21412		42.09	11.20	
	4**	4.18	34	4.38324		53.65	7.76	
	5**	5.21	15	3.33552		66.86	4.50	
	6*	6.10	12	3.01516		78.29	3.98	
	7	7.17	-	3.15001		-	-	
	8	8.21	22	3.22872		-	(6.81)	
	9	8.98	17	2.89311		-	(5.88)	
A6 2.0 kg	1	1.12	1780	3.16151	.139	8.07	(563.-)	1.18147
	2*	2.12	547	4.86875		15.27	112.3	
	3*	3.28	155	3.21412		23.63	48.2	
	4**	4.18	131	4.38324		30.11	29.9	
	5**	5.21	45	3.33552		37.53	13.5	
	6*	6.10	42	3.01516		43.94	13.9	
	7	7.17	21	3.15001		-	-	
	8	8.21	32	3.22872		-	(6.7)	
	9	8.98	29	2.89311		-	-	
A11 5.0 kg	1	1.12	893	3.16151	.169	12.52	-	.77039
	2*	2.12	190	4.86875		19.37	183.4	
	3*	3.28	238	3.21412		24.69	59.1	
	4**	4.18	76	4.38324		30.77	54.3	
	5**	5.21	58	3.33552		36.02	22.8	
	6*	6.10	59	3.01516		-	19.2	
	7	7.17	-	3.15001		-	(18.7)	
	8	8.21	85	3.22872		-	(26.3)	
	9	8.98	51	2.89311		-	(17.6)	
A12 15.0 kg	1	1.12	2320	3.16151	.279	7.59	476.5	.26209
	2*	2.12	690	4.86875		11.74	214.7	
	3*	3.28	547	3.21412		14.96	124.8	
	4**	4.18	218	4.38324		18.64	65.4	
	5**	5.21	204	3.33552		21.83	67.7	
	6*	6.10	140	3.01516		-	(44.4)	
	7	7.17	-	3.15001		-	(99.4)	
	8	8.21	321	3.22872		-	(58.1)	
	9	8.98	168	2.89311		-	-	
A14 30.0 kg	1	1.12	4160	3.16151	.337	6.29	854.4	.17530
	2*	2.12	1082	4.86875		9.74	336.6	
	3*	3.28	786	3.21412		12.41	179.3	
	4**	4.18	278	4.38324		15.47	83.4	
	5**	5.21	290	3.33552		18.11	96.2	
	6*	6.10	357	3.01516		-	(113.3)	
	7	7.17	514	3.15001		-	(199.2)	
	8	8.21	274	3.22872		-	(84.7)	
	9	8.98		2.89311				

- 8 -

TABLE V

Shot No.	i	c_i [μ-str/μs]	k_i [μ-str/atm]	a [m]	$\dfrac{a\cdot10^4}{A_o^* C_e}$	ξ_i corr	$\dfrac{c_i\,a}{F_o C_e k_i}$
A4 0.5 kg (O)	1	28.7	3.16151	.06635	2.55364	31.95	2.318·10⁻³
	2	4.17	4.86875			49.43	2.187·10⁻⁴
	3	.50	3.21412			62.99	3.373·10⁻⁵
	4	.46	4.38324			78.52	2.680·10⁻⁵
	5	.22	3.33552			91.93	1.684·10⁻⁵
	6	.32	3.01506				(2.770·10⁻⁵)
	7	*	3.15001				
	8	*					
	9	*					
A5 0.5 kg (●)	1	31.0	3.16151	.07817	3.00817	27.12	2.050·10⁻³
	2	6.55	4.86875			41.96	4.047·10⁻⁴
	3	.86	3.21412			53.48	8.949·10⁻⁵
	4	.56	4.38324			66.65	3.843·10⁻⁵
	5	.21	3.33552			78.04	1.894·10⁻⁵
	6	.32	3.01506				(3.193·10⁻⁵)
	7	*	3.15001				
	8	*					
	9	*					
A6 2.0 kg (□)	1	73.3	3.16151	.13870	5.33797	15.28	1.238·10⁻²
	2	19.2	4.86875			23.65	2.105·10⁻³
	3	4.60	3.21412			30.14	7.640·10⁻⁴
	4	2.95	4.38324			37.56	3.605·10⁻⁴
	5	1.97	3.33552			43.98	1.552·10⁻⁴
	6	1.76	3.01506				(3.116·10⁻⁴)
	7	1.05	3.15001				
	8	.48					
	9						
A11 5.0 kg (■)	1	26.0	3.16151	.16896	6.50234	12.55	3.472·10⁻³
	2	4.39	4.86875			19.41	8.881·10⁻⁴
	3	4.50	3.21412			24.74	6.676·10⁻⁴
	4	1.14	4.38324			30.84	2.222·10⁻⁴
	5	1.37	3.33552			36.10	(2.955·10⁻⁴)
	6	.63	3.01506				
	7	.56	3.15001				
	8	.46					
	9						

TABLE IV

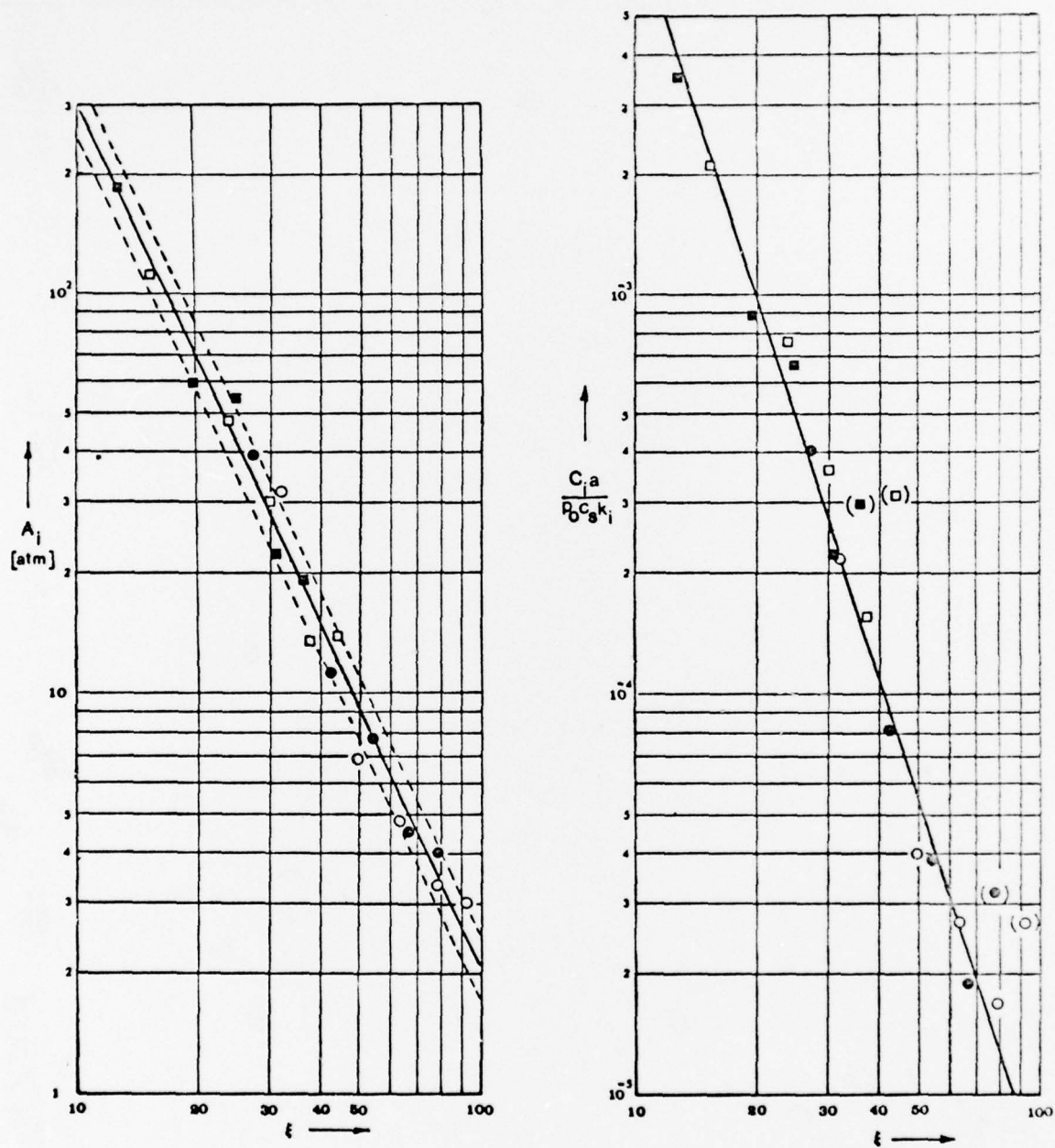| Shot No.	i	d_i [m]	A_i [μ-str]	k_i [μ-str/atm]	a [m]	ξ_i corr	A_i [atm]
A4 0.5 kg (O)	1	1.12	590	3.16151	.06635	31.95	31.84
	2	2.12	155	4.86875		49.43	6.84
	3	3.28	22	3.21412		62.99	4.79
	4	4.18	21	4.38324		78.52	3.30
	5	5.21	11	3.33552		91.93	2.99
	6	6.10	9	3.01506			
	7	7.17	–	3.15001			
	8	8.21	–	3.22872			
	9	8.99	–	2.89311			
A5 0.5 kg (●)	1	1.12	629	3.16151	.07817	27.12	39.02
	2	2.12	190	4.86875		41.96	11.20
	3	3.28	36	3.21412		53.48	7.76
	4	4.18	34	4.38324		66.65	4.50
	5	5.21	15	3.33552		78.04	3.98
	6	6.10	12	3.01506			
	7	7.17	–	3.15001			
	8	8.21	22	3.22872			
	9	8.99	17	2.89311			
A6 2.0 kg (□)	1	1.12	1790	3.16151	.13870	15.28	112.3
	2	2.12	547	4.86875		23.65	48.2
	3	3.28	155	3.21412		30.14	29.9
	4	4.18	131	4.38324		37.56	13.5
	5	5.21	45	3.33552		43.98	13.9
	6	6.10	42	3.01506			
	7	7.17	21	3.15001			
	8	8.21	(32)	3.22872			
	9	8.99	29	2.89311			
A11 5.0 kg (■)	1	1.12	–	3.16151	.16896	12.55	183.4
	2	2.12	893	4.86875		19.41	59.1
	3	3.28	190	3.21412		24.74	54.3
	4	4.18	238	4.38324		30.84	22.8
	5	5.21	76	3.33552		36.10	19.2
	6	6.10	58	3.01506			
	7	7.17	59	3.15001			
	8	8.21	85	3.22872			
	9	8.99	51	2.89311			

Fig.4. The resulting attenuation curves for the maximum amplitude A_i
and for the non-dimensional "dispersion" $C_i a/p_o c_s k_i$
(Half burried charges)

neglected and the evaluation repeated as shown in the Tables IV
and V. Inspection of the data reveals that only data from the
pickups No.2,3,4,5 and 6 can be relied upon. Those data are marked
with a star (*) in the tables.

The results for the six shots as well as for the four
shots are as follows:

<div align="center">

For the 6 shots: For the 4 shots:
(Tables II and III)   (Tables IV and V)

</div>

$$A_o^* = 41576 \text{ [atm]} \qquad\qquad A_o^* = 43765 \text{ [atm]}$$
$$\lambda = -2.15234 \qquad\qquad\qquad \lambda = -2.16719 \qquad (4.8)$$
$$m = \pm17.8\% \qquad\qquad\qquad\quad m = \pm18.5\%$$

$$C_o = 10.88044 \qquad\qquad\quad C_o = 11.83964$$
$$\lambda_a = -3.11369 \qquad\qquad\quad \lambda_a = -3.14128 \qquad (4.9)$$
$$m = \pm24.7\% \qquad\qquad\qquad\quad m = \pm23.6\%$$

For all practical purposes these results may be considered as
identical.

Tables IV and V show the legend used when the result is
plotted in Fig.4 .

Unfortunately the data from the fully confined charges
detonated in B in Fig.1 are not reliable. The reason for rejecting
data from the pickups No.7,8 and 9 in the evaluation of the sur-
face charges was, that the signals showed a behaviour which could
be interpreted as caused by a major crack in the rock between pick-
ups No.6 and 7. In this case the shock wave travels in the oppo-
site direction, and one would expect only data from the pickups
No. 9,8, and 7 to be relevant. The data are plotted in Fig.5 and
it is observed that the wave from the 0.5 kg charge is damped less
than the wave from the 2.0 kg charge. Consequently the smaller
charge creates a larger maximum amplitude in the shock wave
after a certain distance than the larger one, a result which must
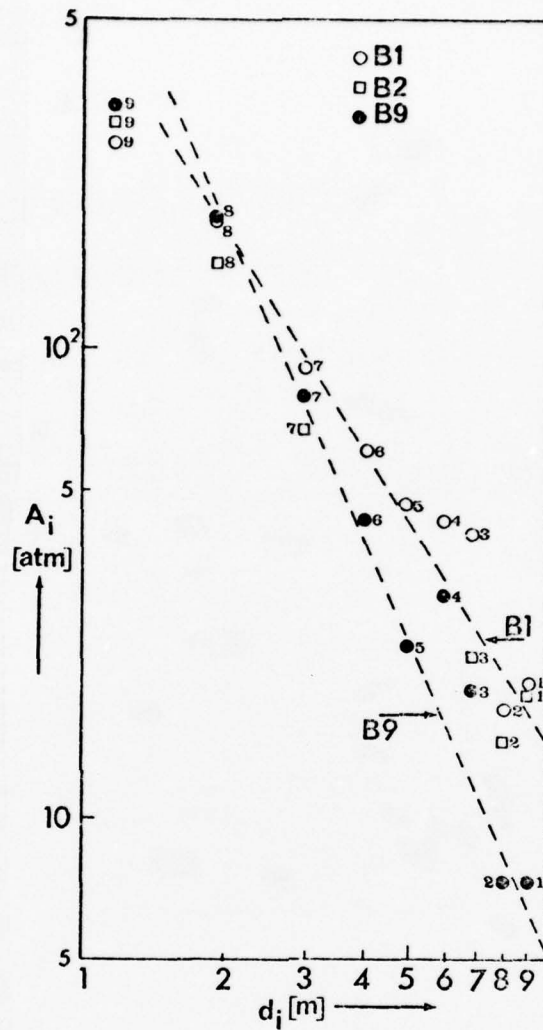be rejected on physical grounds.

Fig. 5. Data from shots B1, B2 and B9 with the
attenuation curves derived from the data
of B1 and B9 seperately.

Difficulties occurred with the charge in shot B2. The data from this shot are therefore neglected. The dashed lines in Fig. 5 show the attenuation curves given by the two shots B1 and B9 seperately. The deviation is so great that further attempts at drawing meaningful conclusions from these data are thought futile. This means that the previously established correlation between the effect of a half buried charge as compared with a fully contained charge could not be checked.

5. The "hole"-experiment, VIKERSUND.

The geometry and the purpose of the "hole"-experiment at Vikersund has already been treated and shown in Fig.2 . Fig.6 shows the 17 strain gauges and their positions relative to the surface of

Fig.6 Positions of the strain gauges in the "hole"-experiment at VIKERSUND given in centimeters from the surface.

the rock. It is noticed that the gauges 5 and 6, 11 and 12, and 14 and 15 are placed opposite each other at the same distance from

TABLE VI

Shot No.	h	Pickup/W	1	2	3	4	5	7	8	9	10	11	13	14	15	16	17	6	12
16	60cm	0.5kg	-	-	10	15	17	24	30	-	44	88	52	448	71	109	114		
17			-	-	12	15	-	16	24	14	37	35	39	357	59	85	125		
18			-	-	12	14	12	19	22	24	40	39	46	381	56	94	134		
19	40cm	0.5kg	12	14	13	14	17	25	30	26	42	50	65	595	94	128	152		
20			11	12	13	18	17	27	33	-	50	63	71	711	99	146	195		
21			11	-	12	14	17	23	34	30	57	58	54	666	94	137	210		
22	90cm	2.0kg	-	-	-	20	22	37	37	51	-	62	60	643	86	125	152		
23			15	15	-	23	26	39	37	35	52	47	46	476	64	109	157		
24			17	13	-	20	20	31	37	37	47	56	56	547	67	118	250		
25	63.5cm	2.0kg	27	27	28	32	34	51	66	61	76	88	89	762	123	187	199		
26			28	29	-	40	32	54	63	61	80	104	87	773	134	170	162		
27			23	26	29	35	29	51	60	57	74	104	103	1035	118	224	379		
28	129cm	5.0kg	25	27	25	33	33	49	60	55	71	75	75	714	96	131	163		
29			22	22	29	32	33	52	57	51	63	59	61	607	96	103	293		
30			23	20	26	27	32	44	49	47	51	51	56	464	80	79	299		
31	86cm	5.0kg	36	31	39	46	50	72	83	76	114	118	112	1000	198	200	466		
32			36	-	42	52	50	78	89	79	128	150	168	1250	225	340	737		
33			34	-	35	41	45	73	73	71	77	129	128	1000	-	256	437		
34	20cm	0.5kg	16	-	16	21	20	30	42	37	66	67	73	857	380	153	876		
35			18	-	17	23	21	34	45	34	68	59	87	857	476	177	1460		
36			13	-	16	21	21	34	42	34	66	67	75	928	465	183	950		
37	32cm	2.0kg	50	43	58	68	-	98	113	116	213	-	310	2237	-	610	-		
38			44	42	53	67	61	92	98	111	456	407	234	2600	-	-	-	63	280
39	43cm	5.0kg	67	62	79	91	95	131	161	158	-	460	-	5600	-	-	-	103	360
40	0cm	0.5kg	86	87	119	140	156	226	256	278	-	927	-	-	-	-	-	180	943
41	-8cm	0.5kg	84	87	105	125	140	-	-	378	-	-	-	-	-	-	-	164	

the surface. The maximum amplitudes of the shock waves measured in [μ-strain] at each strain gauge as well as the specifications of each shot (distance above the surface h and charge magnitude W) are given in TABLE VI.

It is observed that the instrumentation of this experiment is different from the one used in the "row"-experiment. The question of whether or not the type of instrumentation influences the data such that conclusions drawn on the physical behaviour really reflects instrument-induced errors becomes important. It is therefore imperative somehow to connect the results from this experiment with that of the "row"-experiment. This occurs first through the determination of the signal velocity of the rock. In Fig.7 are the arrival times t_a of the signals at the different pickups and the distance d travelled plotted against each other for the shots 16, 18, 20, 37 and 38. The data exhibit a comparatively large scatter,
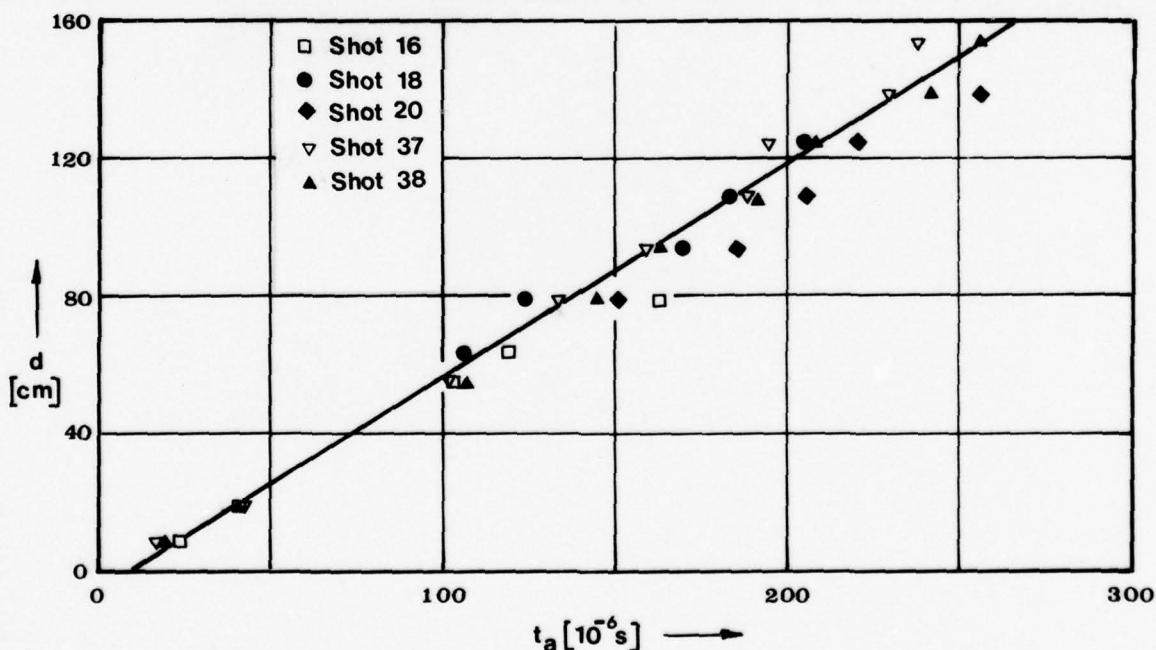
Fig.7 . Arrival time t_a of the shock wave at the pickups related to the distance d travelled. "Hole"-experiment, VIKERSUND:

but the straight line through these points, determined by linear regression, gives through its slope the signal velocity c_s as follows:

$$c_s = 6210 \text{ [m/s]} \qquad , \qquad b = 5.18 \text{ [m]} \qquad (5.1)$$

where b is the distance at which $t = 0$, leaving an impression of the accuracy of the measurements. The agreement between the results (4.3),(4.4) and (5.1) is satisfactory.

The only data in Table VI which may be compared to the results obtained in the "row"-experiment are the ones from the shots 40 and 41. Only in these two cases did one have the charges in contact with the rock's surface. The data are repeated in Table VII which also gives the legend for the points in Fig.8 .

TABLE VII

Shot No.	Pickup i	d_i [cm]	A_i [μ-str]
40	1	190	86
	2	175	87
	3	161	119
	4	145	140
	5	130	156
	6	130	180
	7	115	226
	8	100	256
	9	91	278
	10	80	–
	11	55	927
◇	12	55	943
41	1	190	84
	2	175	81
	3	161	105
	4	145	125
	5	130	140
	6	130	164
	7	115	–
	8	100	–
●	9	91	378

The straight line through the data points will have a slope λ which can be determined by linear regression:

$$\lambda = -1.9779 \qquad (5.2)$$

This value should be compared with the values obtained in (4.8). A better idea of the agreement between the two cases is however obtained by comparing the results in an attenuation diagram. Fig.8 shows this where the fully drawn line represents the attenuation curve determined from the data shown, and the dashed line represents the attenuation curve obtained from the results of the "row"-experiment with $\alpha = 0.06635$ [m] for a charge $W = 0.5$ [kg] and with a mean value of $k = 3.1$ [μ-str/atm]
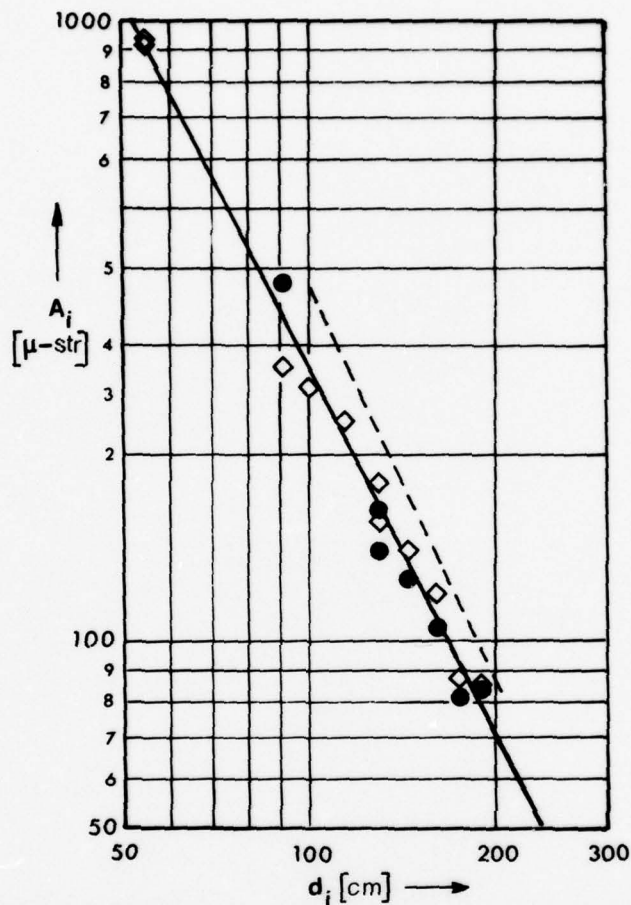
*Fig.8 . Maximum amplitudes A_i ("hole"-experiment)
by the shots 40 and 41.*

for the calibration constant. Considering the fact that one is
in this case comparing results from experiments with two entirely
different types of pickups, the agreement must be considered very
satisfactory.

So far the experiments have dealt with situations for
which at least some sort of theoretical approach could be en-
visaged. For cases with charges detonated in the air above the
surface, no theoretical method known to the author exists by
means of which one can relate the shock wave induced in the ground
to that which the same charge would have caused when detonated
completely confined. The idea behind the experiments was to do
this experimentally.

The free hanging charges will induce shock waves in the rock which will be influenced among other things by the distance h above the surface at which the charge is detonated. This distance may be made dimensionless by scaling it against the charge magnitude W , i.e. $h_* = h/\sqrt[3]{W}$. The experiment was planned such that the non-dimensional distance h_* was repeated for each charge magnitude. One observes that this means equivalence in the way in which distances are scaled in the rock as well as above its surface.

Before examining the experimental data one may contemplate what kind of relationship one may anticipate. If one uses the attenuation curve for the maximum amplitude of the shock wave in the case of fully contained explosions as a guide, one will expect an attenuation curve as shown in Fig.9 , where the maxi-
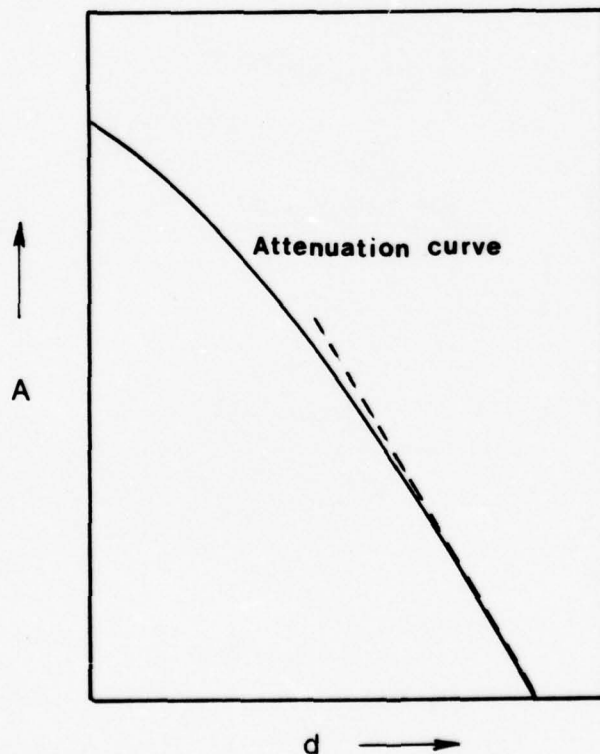
Fig.9 . Attenuation curve for the maximum amplitude A

mum amplitude A is plotted as a function of the distance d travel-

led by the shock wave. The diagram is in doubly logarithmic scale and consequently the curve ought to exhibit an assymptotic behaviour as a straight line as shown by the dashed line.

One may be more specific at this point. One cannot offhand know how the attenuation curve is influenced by the rock type, the type of explosive used, the dimensionless duration τ_o of the input pulse and/or the elevation h above the surface. One can however assume as a working hypothesis that

a) the distances may be scaled with $\sqrt[3]{W}$,

b) the dimensionless duration τ_o is the same in all cases, because among other things the same explosive is used ,

c) the data, which here consists of measured maximum amplitudes of the shock wave, will depend only on one parameter, say h_*.

Such a hypothesis corresponds to the expected behaviour of the attenuation curve for a contained explosion.

This hypothesis is now examined in the two Tables VIII and IX. First Table VIII is arranged in such a way that the three cases of constant h_* appear separately. One then computes the ratios between the measured maximum amplitudes at each pickup. [A_{05} , A_{20} and A_{50} are the maximum amplitudes measured with $W =0.5$[kg] , $W = 2.0$[kg] and $W = 5.0$[kg] respectively.] It is observed that the ratios remain fairly constant for larger distances. The average value of the ratios neglecting those closest to the charge and appearing in paranthesis () in the table is given.

Secondly Table IX is arranged such that the three cases of different charge magnitudes appear separately. Again the ratios are computed and again the average values of the ratios are given for the pickups farthest away from the surface. This exercise indicates that the data should be subjected to a scaling procedure which is exhibited in Fig.10 . On the transparent page 1 the data from the 0.5 kg-charges at different distances h are gathered. The scaling occurs vertically and is proportional to $1/h_*$. On page 2 the same has been done for the 2.0 kg-charges, but here a horizontal scaling occurs in accordance with point a) above. On

TABLE VIII

	$A_{0.5}$	$A_{2.0}$	$A_{5.0}$	$A_{0.5}/A_{2.0}$	$A_{0.5}/A_{5.0}$	Remarks
W	0.5kg	2.0kg	5.0kg			
h/i	60cm	90cm	129cm			
1	-	16.-	23.33			$(A_{0.5}/A_{0.2})_{Av.}$ = 0.6319±0.0631
2	-	14.-	23.-			
3	11.33	-	26.67		.4248	$(A_{0.5}/A_{5.0})_{Av.}$ = 0.4471±0.0274
4	14.67	21.-	30.67	.6986	.4783	
5	14.50	22.67	32.67	.6396	.4438	
6	-					
7	19.67	35.67	48.33	.5514	.4070	
8	25.33	37.-	55.33	.6846	.4578	
9	24.-	41.-	51.-	.5854	.4706	
10	40.33	49.50	61.67	(.8147)	(.6540)	
11	54.-	55.-	61.67	(.9818)	(.8756)	
12						
13	45.57	54.-	64.-	(.8439)	(.7120)	
14	394.67	555.33	595.-	(.7107)	(.6633)	$h_* = 13.60$
15	62.-	72.33	90.67	(.8572)	(.6838)	
16	96.-	117.33	104.33	(.8182)	(.9202)	
17	124.33	186.33	251.67	(.6673)	(.4940)	
h/i	40cm	63.5cm	86cm			
1	11.33	26.-	35.33	.4358	.3207	$(A_{0.5}/A_{2.0})_{Av.}$ = 0.4752±0.036
2	13.-	27.33	31.-	.4757	.4194	
3	12.67	27.50	38.67	.4607	.3276	$(A_{0.5}/A_{5.0})_{Av.}$ = 0.3558±0.035
4	15.33	35.67	46.33	.4298	.3309	
5	17.-	31.67	48.33	.5368	.3517	
6						
7	25.-	52.-	74.33	.4808	.3363	
8	32.33	63.-	83.33	.5132	.3880	
9	28.-	59.67	75.33	.4692	.3717	
10	49.67	76.67	106.33	(.6391)	(.4671)	
11	57.-	98.67	132.33	(.5771)	(.4307)	
12						
13	63.33	93.-	136.-	(.6810)	(.4657)	
14	674.-	856.67	1083.33	(.7868)	(.6222)	
15	95.67	125.-	211.50	(.7654)	(.4523)	$h_* = 9.09$
16	137.-	193.67	265.33	(.7074)	(.5163)	
17	185.67	246.67	546.67	(.7527)	(.3396)	
h/i	20cm	32cm	43cm			
1	15.67	47.-	67.-	.3334	.2339	$(A_{0.5}/A_{2.0})_{Av.}$ = 0.3389±0.0352
2	-	45.-	62.-			
3	16.33	55.50	79.-	.2942	.2067	$(A_{0.5}/A_{5.0})_{Av.}$ = .2335±0.0205
4	21.67	67.50	91.-	.3210	.2381	
5	20.67	61.-	95.-	.3389	.2176	
6		63.-	103.-			
7	32.67	95.-	131.-	.3439	.2494	
8	43.-	105.5	161.-	.4076	.2671	
9	35.-	113.5	158.-	.3084	.2215	
10	66.67	334.5	-	(.1993)		
11	64.33	407.-	460.-	(.1581)	(.1398)	
12		280.-	360.-			
13	78.33	272.-	-	(.2880)		
14	880.67	2418.50	5600.-	.3641	(.1573)	$h_* = 4.54$
15	440.33	-	-			
16	171.-	610.-	-	(.2803)		
17	1098.67	-	-			

page 3 the same procedure is repeated for the data from the *5.0 kg*-charges. Because the pages are transparent the figure reveals how nicely the data seem to follow the scaling laws outlined above.
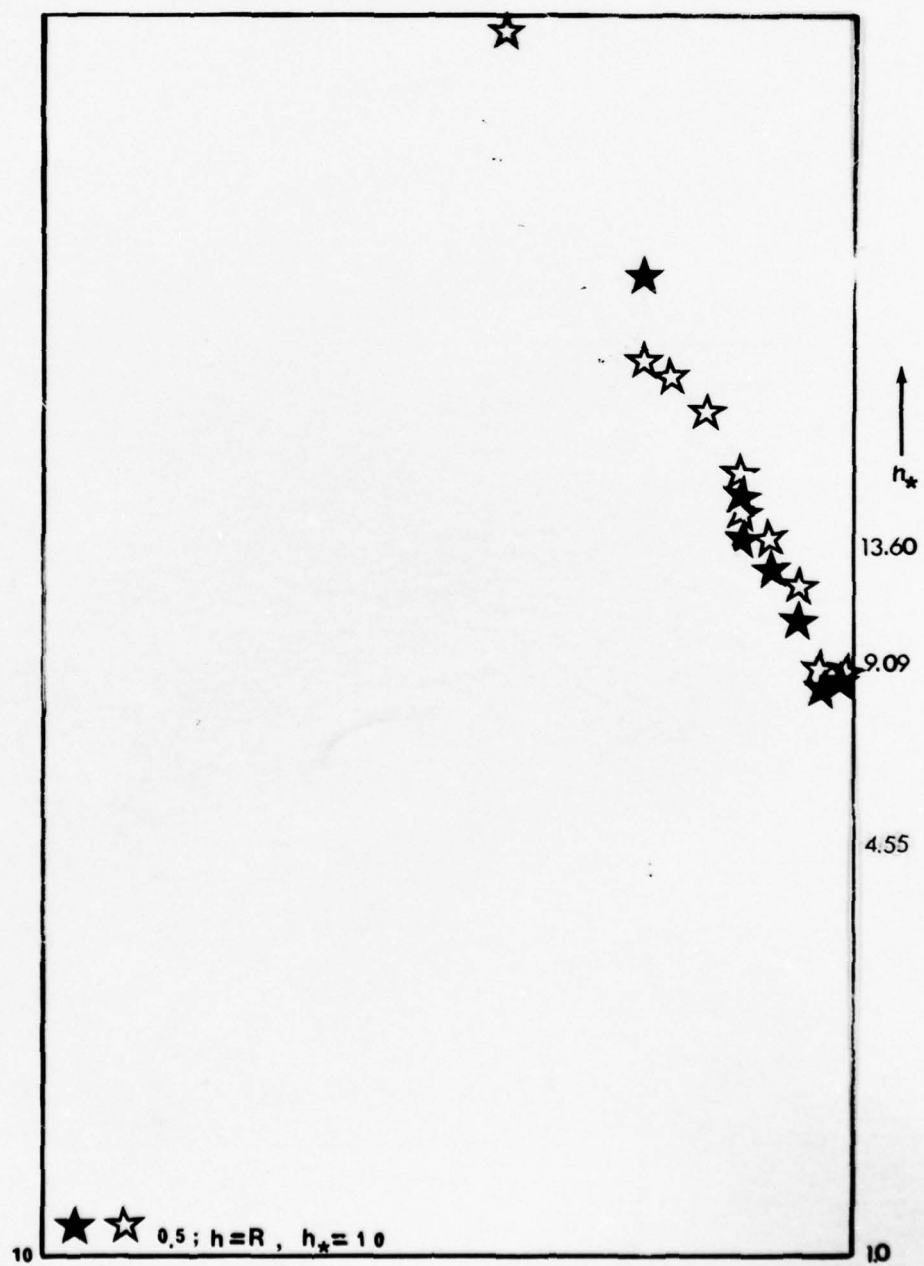
One should at this point add the following remarks:
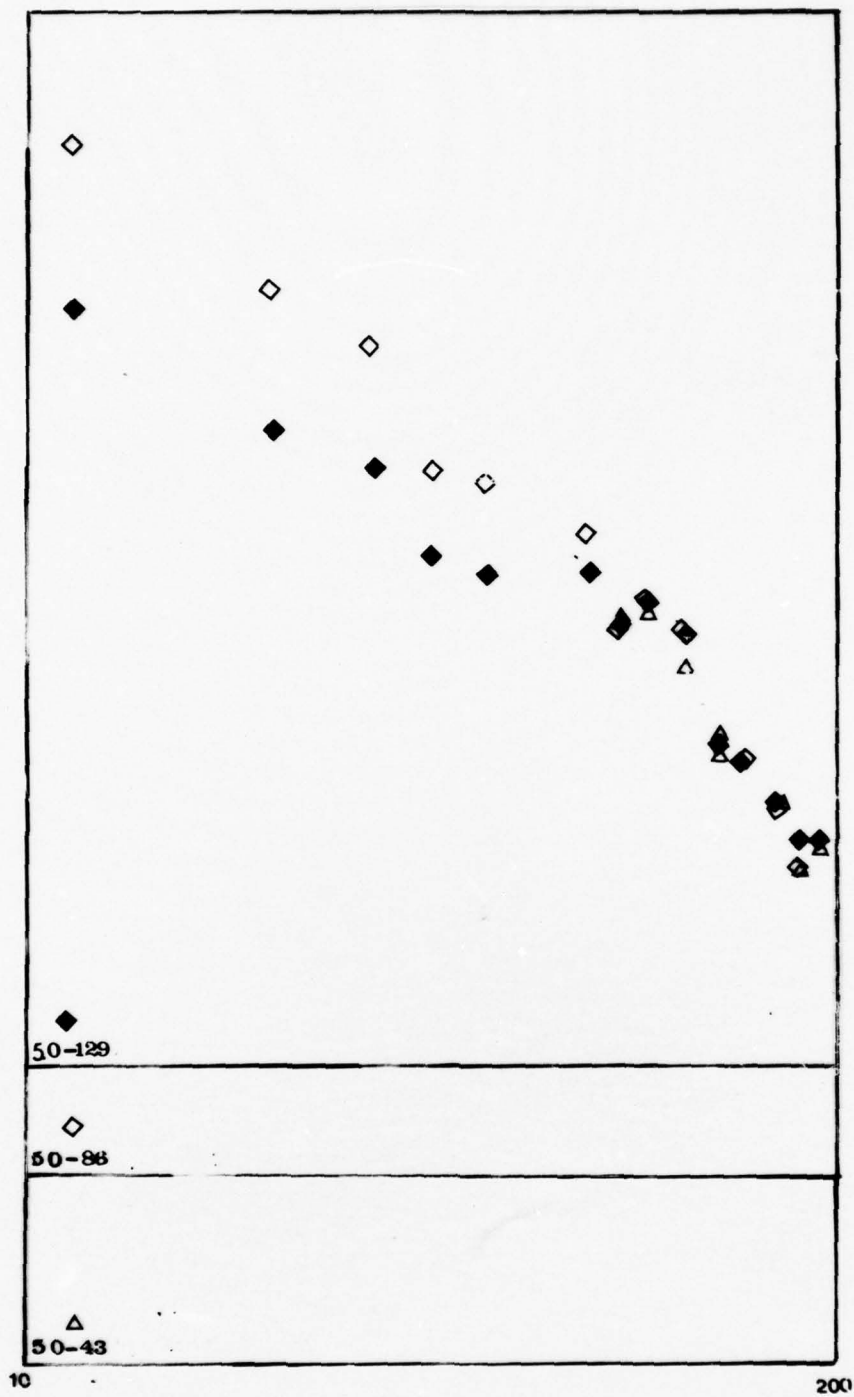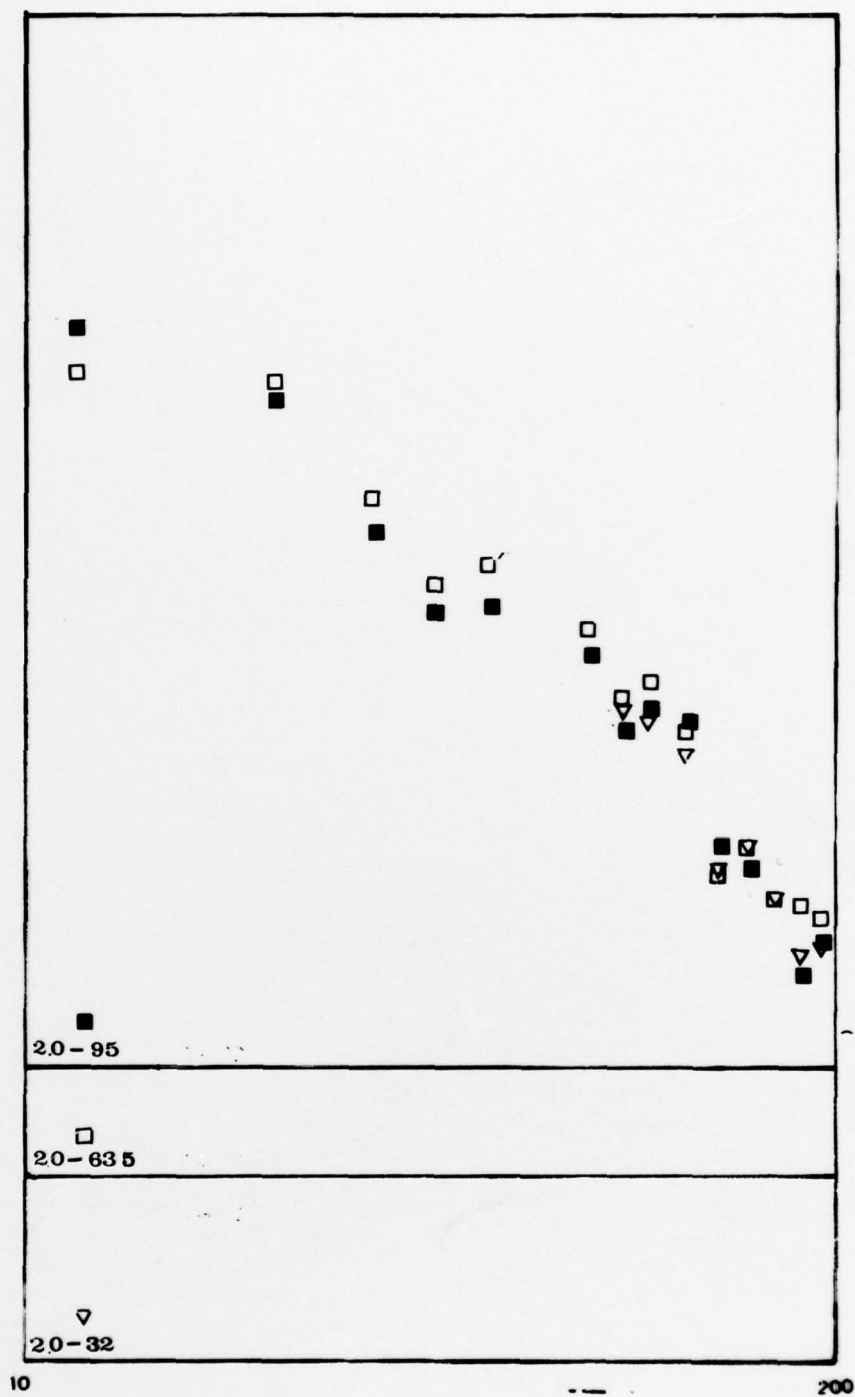The ratios computed may to some extent be independent of eventual

TABLE IX

W	i	d_i	h_1 A_{1i}	h_2 A_{2i}	h_3 A_{3i}	A_{1i}/A_{2i}	A_{1i}/A_{3i}	Remarks
0.5 kg	1	190	-	11.33	15.67			A_{1i}/A_{2i}=0.8554±0.066
	2	175	-	13.-	-			
	3	161	11.33	12.67	16.33	.8942	.6938	A_{1i}/A_{3i}=0.6511±0.052
	4	145	14.67	15.33	21.67	.9569	.6770	
	5	130	14.50	17.-	20.67	.8529	.7015	
	6	130						
	7	115	19.67	25.-	32.67	.7868	.6021	h_1 = 60cm
	8	100	25.33	32.33	43.-	.7835	.5891	h_2 = 40cm
	9	91	24.-	28.-	35.-	.8571	.6857	h_3 = 20cm
	10	80	40.33	49.67	66.67	(.8120)	(.6049)	
	11	55	54.-	57.-	64.33	(.9474)	(.8394)	
	12	55						
	13	45	45.57	63.33	78.33	(.7196)	(.5818)	
	14	36	394.67	674.-	880.67	(.5856)	(.4481)	
	15	36	62.-	95.67	440.33	(.6481)	(.1408)	
	16	25	96.-	137.-	171.-	(.7007)	(.5614)	
	17	12	124.33	185.67	1098.67	(.6696)	(.1132)	
2.0 kg	1	190	16.-	26.-	47.-	.6154	.3404	A_{1i}/A_{2i}=0.6275±0.072
	2	175	14.-	27.33	45.-	.5123	.3111	
	3	161	-	27.50	55.50	-	.3111	A_{1i}/A_{3i}=0.3460±0.027
	4	145	21.-	35.67	67.50	.5887	.3716	
	5	130	22.67	31.67	61.-	.7158		
	6	130			63.-	-		
	7	115	35.67	52.-	95.-	.6860	.3755	h_1 = 90cm
	8	100	37.-	63.-	105.50	.5873	.3507	h_2 = 63.5cm
	9	91	41.-	59.67	113.50	.6871	.3612	h_3 = 32cm
	10	80	49.50	76.67	334.50	(.6456)	(.1480)	
	11	55	55.-	98.67	407.-	(.5574)	(.1351)	
	12	55			280.-	-		
	13	45	54.-	93.-	272.-	(.5806)	(.1985)	
	14	36	555.33	856.67	2418.50	(.6482)	(.2296)	
	15	36	72.33	125.-	-	(.5786)		
	16	25	117.33	193.67	610.-	(.6058)	(.1923)	
	17	12	186.33	246.67	-	(.7554)		
5.0 kg	1	190	23.33	35.33	67.-	.6603	.3482	A_{1i}/A_{2i}=0.6776±0.029
	2	175	23.-	31.-	62.-	.7419	.3710	
	3	161	26.67	38.67	79.-	.6897	.3376	A_{1i}/A_{3i}=0.3466±0.016
	4	145	30.67	46.33	91.-	.6620	.3370	
	5	130	32.67	48.33	95.-	.6760	.3439	
	6	130			103.-			
	7	115	48.33	74.33	131.-	.6502	.3689	h_1 = 129cm
	8	100	55.33	83.33	161.-	.6640	.3437	h_2 = 86cm
	9	91	51.-	75.33	158.-	.6770	.3228	h_3 = 43cm
	10	80	61.67	106.33	-	(.5800)	-	
	11	55	61.67	132.33	460.-	(.4660)	(.1341)	
	12	55			360.-			
	13	45	64.-	136.-	-	(.4706)		
	14	36	595.-	1083.33	5600.-	(.5492)	(.1063)	
	15	36	90.67	211.50		(.4287)		
	16	25	104.33	265.33		(.3932)		
	17	12	251.67	546.67		(.4604)		

systematic errors in the data. An example is the data from pick-up no. 14 which evidently are erroneous. Still the ratio computed from them is not unrealistic. This means further that even though the data give ratios with fair degree of accuracy (<10%) they may still exhibit a rather large scatter. Fig.10 shows how this is the case for data obtained close to the surface.

0,5 ; h=R , $h_* = 1\,0$
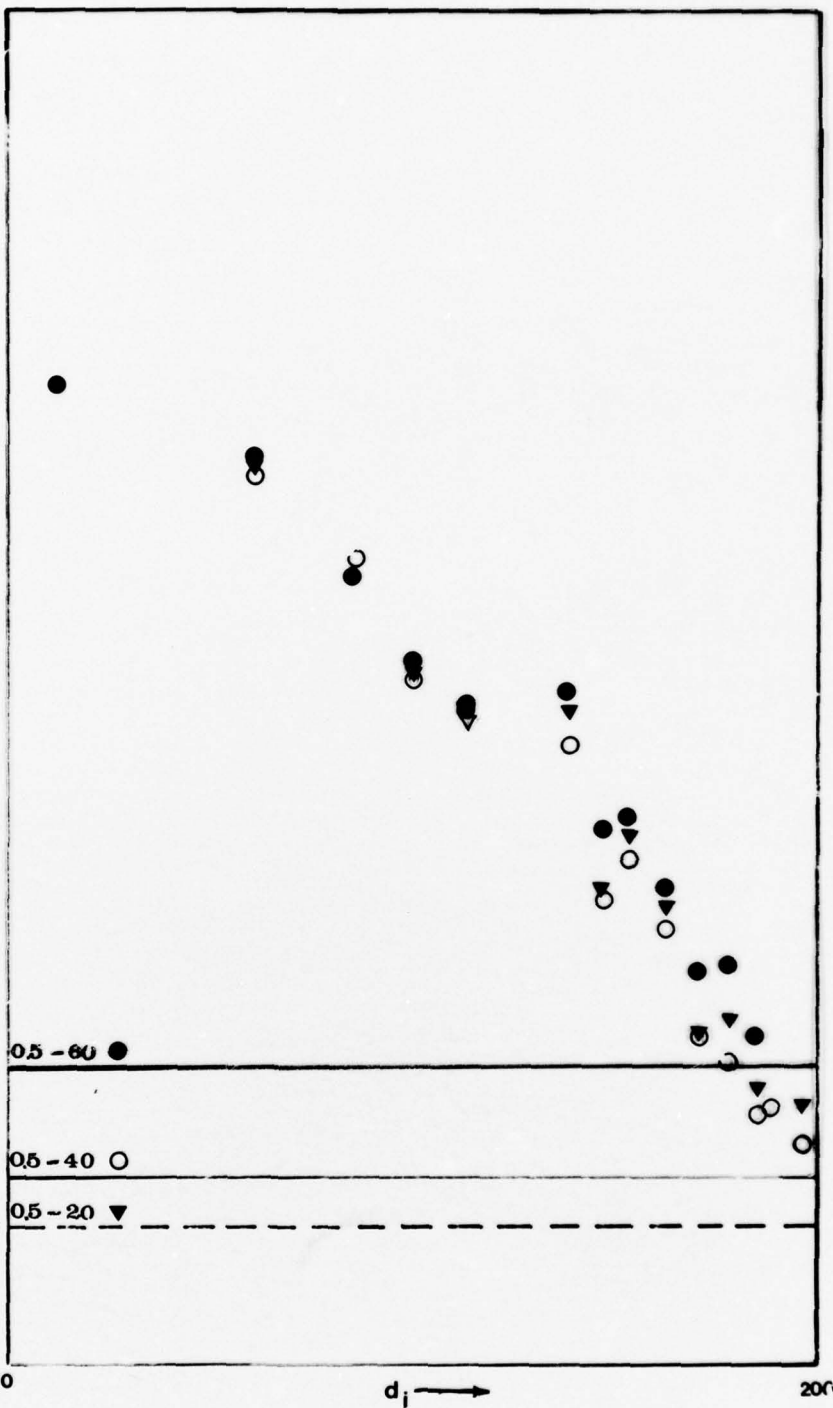
Page 4

2.0 – 95

2.0 – 63 5

2.0 – 32

10   200

A_i

$0.5 - 60$ ●

$0.5 - 40$ ○

$0.5 - 20$ ▼

10

10

10

10

10

$d_i \longrightarrow$

200

Fig.10. Correlation of all measured
maximum amplitudes A_i.

It must be remarked that the data for the case of $W = 0.5\ kg$ and $h = 20\ cm$ do not seem to fit in with the proposed scaling procedure. It is therefore plotted in with its base line dashed.

Finally it should be remarked that the exercise so far has only given a scaling procedure for cases of free hanging charges. If it is extended to the case of the charge in contact with the surface, ($h_* = 1$), one would have been able to connect the present result to the case of half buried charges and thus, through the results of [3], also to the case of a confined charge. In Fig.10 the data from shots 40 and 41 are plotted on page 4 realizing that these data may be regarded as a case for which $h_* = 1$, whereas the other cases give values of this parameter as shown in Table VIII . The fact that these data fit in so nicely with the rest may be taken as a very strong indication that the scaling procedure outlined here may be acceptable.

6. Conclusions from the VIKERSUND experiments.

It is not easy to draw general conclusions from experiments within a limited range. Keeping this in mind one is however encouraged by the apparent consistency in the data and an attempt may be made to generalize the results as follows:

① When comparing two cases I and II where the charges W_I and W_{II} are being detonated in the same distance h_* above the surface of the rock, one will find that the same maximum amplitude in the shock wave is created at distances d_I and d_{II} respectively, whereby

$$d_I = d_{II} \sqrt[3]{\frac{W_I}{W_{II}}} \qquad (6.1)$$

(Maximum amplitude measured in [μ-strain])

This is to be considered the first part of a "scaling law" or a "model law". The non-dimensional distance h_* used here is defined

as

$$h_* = h/R \qquad , \qquad R = \sqrt[3]{3W/4\pi\rho}$$ (6.2)

where h is the elevation above the surface where the detonation takes place, and R is the radius of the equivalent sperical charge with ρ as the density of the explosive..

The second part of the "scaling law" may be formulated as follows:

When comparing two cases I and II where the same charge W is detonated at the non-dimensional elevations $h_{*,I}$ and $h_{*,II}$ respectively, one will find that in the same non-dimensional distance from the surface the shock wave will exhibit maximum amplitudes S_I and S_{II} respectively which will be related to each other through

$$S_I = S_{II} \frac{h_{*,II}}{h_{*,I}}$$ (6.3)

If this result can be substantiated and confirmed by further experimental evidence, one has succeeded in relating at least one important case of air blast induced shock waves in rock to the case of a confined explosion. For cases where crater building is a major factor in the process, reference is being made to the handling of this problem in [3] .

7. The CENSE experiments.

        In connection with the VIKERSUND experiments,
which were conducted on a small scale, it may be of interest to
examine the results of the CENSE experiments. These were conducted
with charges which were orders of magnitude greater. The results
from these experiments are discussed in [2] and the lay-out of
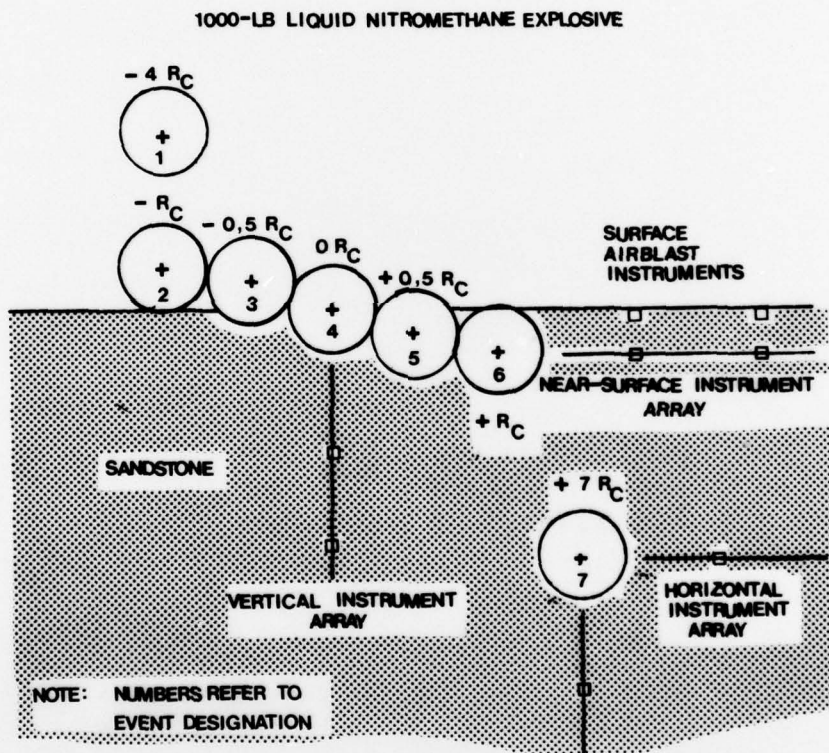the experiments is shown in Fig.11 . The numbers indicate the 7

Fig.11. The experimental lay-out of the CENSE experiments.

different events, where for each event the position of the deton-
ating charge is changed. In this way one covers the whole range of
positions above, on, near to and below the surface. For each event
recordings of the induced shock wave in the rock were made

on a vertical ray through the center of the charge as indicated
through the vertical instrument array. In case 7 also a horizon-
tal instrument array was in operation. Other measurements were
also made, but these are so far of marginal interest in the pre-
sent context.

It should be mentioned that the results of
these experiments, as they appear in [2], are given in terms of
coupling factors. As an example: the ground shock factor F_u is
defined as

$$F_u = \frac{peak\ horizontal\ particle\ velocity}{peak\ radial\ velocity\ for\ full\ containment\ (DoB = 7R_c)} \quad (7.1)$$

It is stressed that the ground shock factor is determine' from
measurements along the near surface instrument radial, and that
data from the measurements directly beneath the explosive are
not included in the analysis. This is in contrast to the present
examination, where only the data from the vertical instrument
array will be used. (In event 7 also the horizontal array will
be considered.)

8. Peak velocity data from the CENSE I experiment.

The data from CENSE I are presented in the
form of recorded particle velocity as function of time as
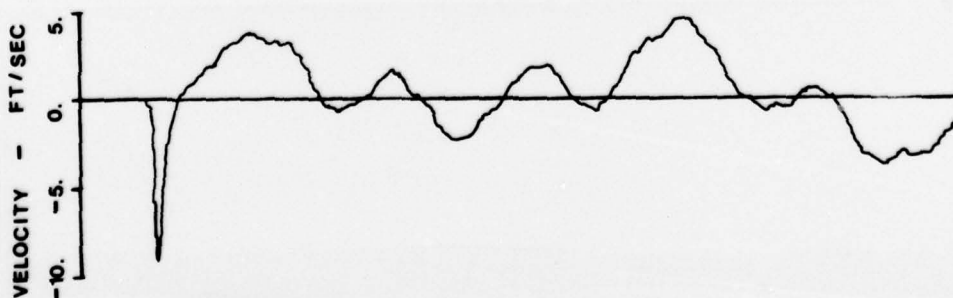examplified in Fig.12 . The peak particle velocity is rather

Fig. 12.   Recorded particle velocity at a distance of 20 feet
          in Event 3.

easily picked out from such recordings, and this quantity is used to characterize the shock waves as done also in the first report [2]. These data are listed in Table X as the maximum amplitude A_i measured at pickup no. i in a distance d_i from the explosion.
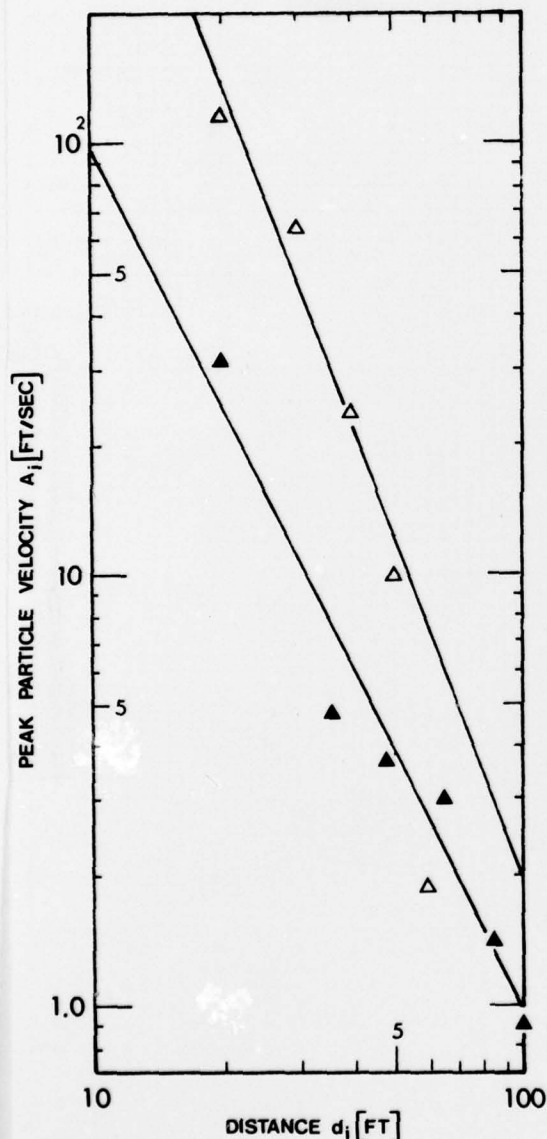
One may start examining these data by looking at the fully contained case, event 7. This is to be a reference case and it is imperative that this case is well established. If the data are plotted as done in Fig.12 , it becomes however apparent that the attenuation of the maximum amplitude of the shock wave is much greater in the vertical than in the horizontal direction. This may indicate that the rock (sandstone) exhibits different properties as a wave-transmitting medium in the two directions, i.e. the sandstone is "layered". Or it may reflect the fact that one or more of the pickups used exhibit systematic errors. Because repeated experiments were not undertaken, and no other information is available, the question of which of the two possibilities is really the case must remain unresolved.

Both data from the horizontal and from the vertical array in event 7 record what may be assumed to be a sherical wave. The idea behind the handling of the data from

Fig. 12. Data from event 7.

TABLE X

Event No.	Pickup i	d_i [ft]	A_i [ft/sec]	F_u	F_u^*	Remarks
1	3	40	.463	.019	.359	Vertical
	4	50	.219	.022	.264	array
O	5	60	.147	.079	.352	
2	1	20	1.767	.015	.078	
	2	30	.514	.008	.101	Vertical
	3	40	(.432)	(.018)	(.335)	array
	4	50	.170	.017	.205	
●	5	60	.112	.060	.268	
3	1	20	9.32	.080	.412	
	2	30	3.184	.051	.624	Vertical
	3	40	.844	.035	.654	
	4	50	.192	.019	.232	array
□	5	60	.156	.084	.373	
4	1	20	12.85	.110	.568	
	2	30	6.077	.096	1.192	Vertical
	3	40	.836	.035	.648	
	4	50	.620	.062	.749	array
■	5	60	.200	.107	.478	
5	1	20	22.64	.194	1.0	
	2	30	5.10	.081	1.0	
	3	40	1.29	.054	1.0	Vertical
	4	50	.828	.083	1.0	
◇	5	60	.418	.224	1.0	array
6	1	20	131.-	1.122		
	2	30	15.5	.246		
	3	40	2.203	.092		Vertical
	4	50	2.452	.245		array
◆	5	60	.722	.388		
7	1	20	116.75	1.0		
	2	30	63.05	1.0		Vertical
	3	40	24.04	1.0		array
	4	50	10.-	1.0		
△	5	60	1.863	1.0		
	6	20	31.78			
	7	36	4.726			
	8	48	3.688			Horizontal
	9	65	2.955			array
	10	85	1.411			
▲	11	100	.891			

the charges placed on or near to the surface is to assume that
the situation on the vertical through the charge can be compared
with the confined case. Now, the confined case appears to give
ambiguous informations, and the reference case thus becomes un-
certain.

In [2] the ground shock factor F_u is defined
in accordance with (7.1) where the data from the horizontal ar-
ray are used for the reference case. If a straight line is fit-
ted through the data points (▲) from the horizontal array in
Fig.12 , an approximation to the attenuation curve is obtained
which may be expressed as

$$A = 10752 \; d_i^{-2.03053} \; [\text{ft/sec}] \qquad (8.1)$$

where A is the peak particle velocity of the shock wave. The
mean deviation of the data points from this line is ±35.7%.

The slope λ of the attenuation curve determined
from the data of the horizontal array above is equal to the ex-
ponent -2.03053 in the expression (8.1). The corresponding slope
determined from the data of the vertical array (△) in Fig.12
is much greater. Even if the point originating from pickup no.5
is neglected as a stray point, the value of the slope would
be

$$\lambda = -2.66817 \qquad (8.2)$$

and the mean deviation of the points from the straight line
shown in Fig.12 would be ±32.6%. The difference in magnitude
of the slopes as well as the vertical position of the straight
lines representing the attenuation curves in Fig.12 is clearly
brought out by the plot. One has however a possibility to check
this result by drawing Fig.3 of the report [2] to attention.
This figure is reproduced in Fig.13 with the original figure
caption. It is seen that the different cases give lines of ap-
proximately the same slope $\lambda \approx -1.55$. This indicates that the
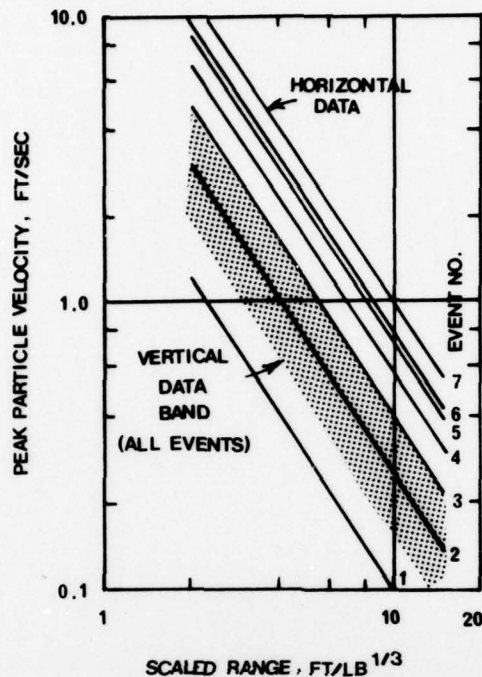present investigation may be based on data which differ from

Fig.13. Replot of Fig.3 in reference [2] with the caption:"Peak particle velocity versus scaled range as a function of charge containment".

those used in reference [2]. It should however be noted, that the magnitude of the slope in Fig.13 corresponds well to the slope $\lambda = -1.65$ suggested by Fred M. Sauer in Nuclear Geoplosics [4] for the socalled composite attenuation curve, and that the slopes obtained from the present data in (8.1) and (8.2) seem unusually high by comparison.

In spite of the discrepancy which seem to have been discovered, it may well be that the data give adequate results for the ground shock factor F_u as defined in (7.1). This factor is therefore computed for each shot and each distance in Table X. Also the factor F_u^* with the data from event 5 as reference has been calculated in the same table. Both cases reveal that no obvious trend can be found in these results.

TABLE XI

Event j	i	d_i [ft]	A_i [ft/sec]	β_j	$\beta_j A_i$ [ft/sec]
1	3	40	.463	1.82616	.846
	4	50	.219		.400
○	5	60	.147		.268
2	1	20	1.767	2.22640	3.934
	2	30	.514		1.144
	3	40	(.432)		.962
	4	50	.170		.378
●	5	60	.112		.249
3	1	20	9.32	1.53131	14.27
	2	30	3.184		4.876
	3	40	.844		1.292
	4	50	.192		.294
□	5	60	.156		.239
4	1	20	12.85	.95670	12.29
	2	30	6.077		5.81
	3	40	.836		.800
	4	50	.620		.593
■	5	60	.200		.191
5	1	20	22.64	.58801	13.313
	2	30	5.10		2.999
	3	40	1.29		.759
	4	50	.828		.487
◇	5	60	.418		.246
6	1	20	131.00	.28552	37.40
	2	30	15.50		4.425
	3	40	2.203		.629
	4	50	2.452		.700
◆	5	60	.722		.206

In spite of this rather discouraging result, one may attempt to establish the ground shock factors by introduction of the "shot factors" β_j as shown in [3] and then determine these by means of the method of the least squares. The result is shown in Table XI where the data from Event 7 have been disregarded entirely. The result ought to be such that the data $(d_i , \beta_j A_i)$, when exhibited in an attenuation diagram , would gather around a straight line with the slope λ. In the present case the calculation is based on the data from the pickups 3 ,4 and 5 only, and the result is shown in Fig.14 . The slope λ of the straight line and the mean deviation m of the points from this line will be
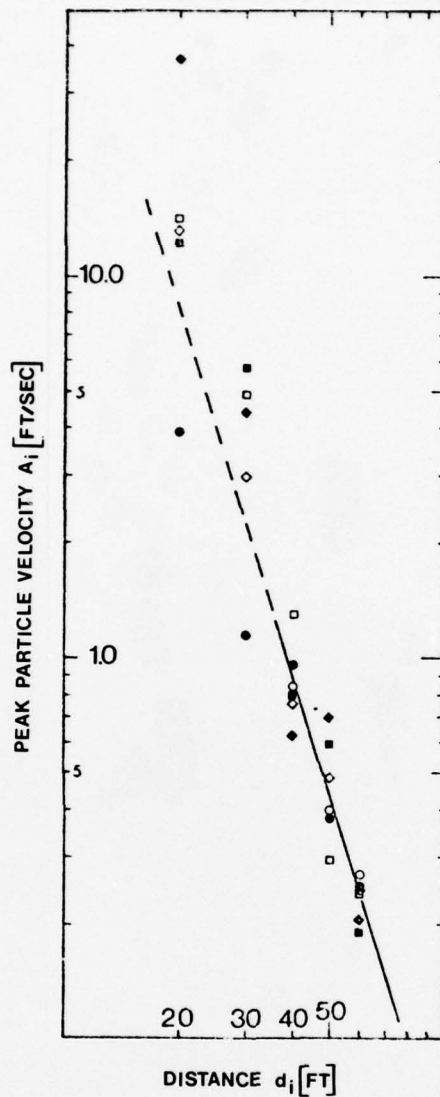
Fig.14 . Corrected data $\beta_j A_i$ plotted as function of
the distance d_i. The straight line repre-
sents the attenuation curve for particle
velocity.

$$\lambda = -3.21792 \qquad , \qquad m = \pm 27.0\% \qquad (8.3)$$

It should be noted that the scatter indicated by m only reflects
the deviation of the data from the pickups 3 , 4 and 5. Fig.14
reveals a much greater scatter as far as the data from pickups
no. 1 and 2 are concerned.

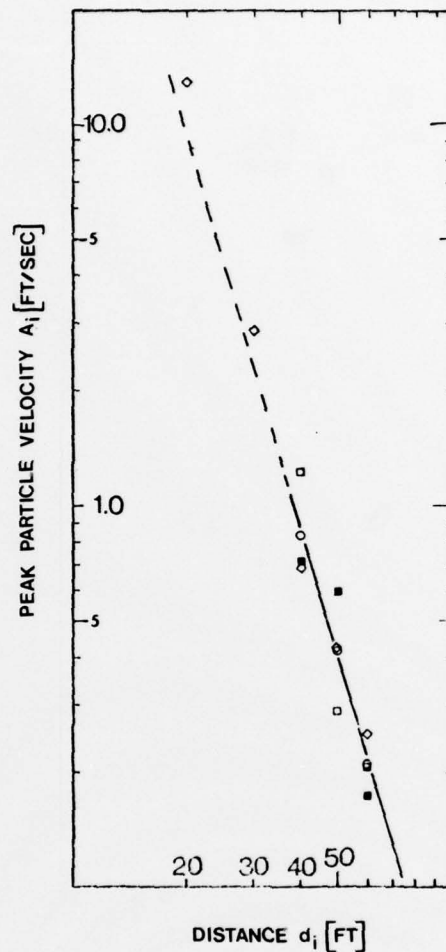| Event j	i	A_i [ft/sec]	B_i [ft/sec]	β_j	$\beta_j \cdot B_i$ [ft/sec]	d_i [ft]
1	3	.463	.500	1.68912	.845	40
	4	.219	.248		.419	50
○	5	.147	.125		.211	60
2	1	1.767	1.600			20
	2	.514	*			30
	3	.432	.800			40
	4	.170	.233			50
●	5	.112	–			60
3	1	9.32	–	1.45665	–	20
	2	3.184	–		–	30
	3	.844	.851		1.24	40
	4	.192	.200		.291	50
□	5	.156	.142		.207	60
4	1	12.85	–	.82302		20
	2	6.077	–			30
	3	.836	.867		.714	40
	4	.620	.729		.600	50
■	5	.200	.212		.174	60
5	1	22.64	26.25	.49382	12.96	20
	2	5.10	5.94		2.93	30
	3	1.294	1.399		.691	40
	4	.828	.866		.428	50
◇	5	.418	.512		.253	60
6	1	131.00	134.36			20
	2	15.50	–			30
	3	2.203	*			40
	4	2.452	*			50
◆	5	.722	.721			60
7	1	(116.75)	–			20
△	2	63.05	69.80			30
	3	(24.04)	*			40
	4	(10.00)	*			50
	5	1.863	1.83			60
▲	6	31.78	–			20
	7	4.726	4.31			36
	8	3.688	*			48
	9	2.955	*			65
	10	1.411	*			85
	11	.891	*			100

Fig.15 . Corrected data $\beta_j B_i$ plotted as function of
the distance d_i. The straight line repre-
sents the attenuation curve for particle
velocity.

It must be mentioned that the data can be obtained
from a second set of curves, which is given with the first one.
This set is not as complete as the first one, the peak particle
velocities obtained from it are denoted by B_i , and they are
given in Table XII, where for comparison the data A_i are repeated.
Missing information is denoted by a star (*) in the table, and
illegible signals with a bar (-).

The same procedure as before leads to the "shot fac-
tors" β_j in Table XII and the attenuation curve is shown in Fig.15.

The slope λ of the straight line and *the mean deviation m* of the data points from this line are

$$\lambda = -3.43792 \qquad , \qquad m = 26.7\% \qquad (8.4)$$

The scatter is about the same as in the case of the first data, the slope λ is also about the same, but in both cases are the values (8.3) and (8.4) much greater than what was obtained in (8.2) and (8.1). All cases give greater values for λ than what is exhibited in Fig.13.

TABLE XIII

Event	The ground shock factor F_u					
	From [2]	From XI	From [2]	From XII	From [2]	From XI
1	.100	.156	.127	.292	.142	.322
2	.247	.128	.315		.351	.264
3	.398	.186	.507	.339	.566	.384
4	.566	.298	.722	.600	.805	.615
5	.703	.486	.896	1.000	1.000	1.000
6	.785	1.000	1.000			
7	1.000					

Finally the ground shock factor F_u is found from Fig.13 and given in Table XIII with Event 7 as basis. If Event 6 is used as basis, the factors will change as shown and compared with the factors which can be computed from the β_j-values of Table XI. With Event 5 as basis, it is possible to compare the factors from [2] with those computed from the β_j-values of both Table XI and XII. Even though the latter two agree reasonably well, it must be concluded that the data upon which the present investigation is based do not give results which conform with those reported earlier [2] from the same experiment.

9. Final remarks

The CENSE experiment distinguishes itself from the

VIKERSUND experiment in the basic philosophy upon which it is planned. The CENSE experiment considers cases where the detonating charge may be placed al all possible levels above as well as below the ground surface. It is assumed that the shock waves created in these cases can be related to each other and/or to the fully contained case by a ground shock factor.

The VIKERSUND experiment is based on the philosophy that a physically important difference exists between cases in which the shock wave is created in connection with a crater formation and cases where this is not the case. The VIKERSUND experiment thus concentrates entirely on cases where the charge is detonated above the surface or in contact with it. The case of the socalled half-buried charge is considered separately in [3], and in spite of the inadequate experimental support, it is believed that a way is suggested whereby the properties of the rock both as a wave-transmitting medium and its ability to withstand cratering is taken into account.

Because of this situation, the two experiments considered in this report do not cover the same physical situations. It could beforehand be expected, that they might in some way compliment each other, but the discrepancies discovered prevent that.

The final result as far as the VIKERSUND experiment is concerned is thus contained in the two statements ① and ②, equations (6.1) and (6.3). It should be emphasized, that further experimentation seems necessary to furnish an adequate experimental support for these results.

10. Acknowledgements.

REFERENCES

[1] Leif N. Persen, "Über die bei Oberflächendetonationen erzeug-
ten Stosswellen im Felsen", Report from
NORCONSULT A/S, Oslo,Norway, Nov.1975

[2] James K. Ingram,"Influence of Burst Position on Airblast,
James L. Drake,   Ground Shock, and Cratering in Sandstone"
Leo F. Ingram   Final Report May 1975, Weapons Effects Labo-
ratory, U.S.Army Engineer Waterways Station,
Vicksburg, Miss. Misc. Paper N-75-3.

[3] Leif N. Persen, "Rock Dynamics and Geophysical Exploration",
Elsevier Scientific Publishing Co., New York,
1975.

[4] Fred M. Sauer, Nuclear Geoplosics, Part IV, "Empirical
Analysis of Ground Motion and Cratering",
DASA-1285 (IV),May 1964, pp. 29 - 64.